Available online at www.CivileJournal.org

Civil Engineering Journal

(E-ISSN: 2476-3055; ISSN: 2676-6957)

Vol. 11, No. 06, June, 2025

Rehabilitation of Partially Corrosion-Damaged Post-Tensioned Concrete Structures Using Carbon Fiber Reinforced Polymer

Hadif Alsuwaidi [1], Ahed Habib [2*], Zaid A. Al-Sadoon [1], Mohamed Maalej [1], Salah Altoubat [1], Samer Barakat [1], M. Talha Junaid [1]

[1] *Department of Civil and Environmental Engineering, College of Engineering, University of Sharjah, P.O. Box. 27272, United Arab Emirates.*

[2] *Research Institute of Sciences and Engineering, University of Sharjah, P.O. Box. 27272, United Arab Emirates.*

Received 24 February 2025; Revised 21 May 2025; Accepted 26 May 2025; Published 01 June 2025

Abstract

This study provides a comprehensive assessment of the deterioration and rehabilitation of post-tensioned (PT) concrete structures affected by chloride-induced corrosion. Through a detailed case study in the United Arab Emirates, the research identifies moisture ingress and inadequate waterproofing as primary contributors to corrosion in PT tendons and ducts, significantly compromising structural integrity. A rigorous evaluation using nondestructive and semi-destructive testing techniques was conducted to quantify damage and determine the extent of degradation. The results revealed severe corrosion in critical structural elements, necessitating targeted intervention to restore performance and durability. To address these challenges, an integrated rehabilitation strategy was developed, incorporating structural repairs, strengthening through carbon fiber-reinforced polymer (CFRP), and advanced waterproofing techniques. The adopted approach involved enlarging load-bearing components and applying CFRP to enhance flexural strength while minimizing aesthetic alterations. Experimental findings demonstrated that CFRP reinforcement increased slab flexural strength by 30% and reduced crack widths by 23%, effectively mitigating corrosion-related deterioration and extending service life. Furthermore, micro-concrete was utilized in all enlargement locations in compliance with ACI standards, ensuring long-term durability. The proposed rehabilitation framework offers a sustainable solution for extending the service life of PT structures exposed to aggressive environmental conditions. By addressing both immediate structural deficiencies and underlying degradation mechanisms, the strategy enhances resilience and reduces future maintenance requirements. The integration of CFRP strengthening, epoxy crack injection, and advanced waterproofing measures significantly improves corrosion resistance and structural longevity.

Keywords: Post-Tensioned Concrete; Corrosion; Chloride Attack; Structural Rehabilitation; CFRP; Durability Enhancement.

1. Introduction

Post-tensioned (PT) concrete structures play a critical role in modern construction, providing enhanced durability and the ability to span greater distances than traditional reinforced concrete systems. The PT method applies a pre-compressive force to the concrete, counteracting tensile stresses induced by service loads and improving structural capacity and serviceability [1, 2]. Despite these advantages, PT structures remain vulnerable to long-term deterioration, mainly due to the condition of steel tendons, which are essential for maintaining pre-compressive forces [3]. One of the most significant challenges in preserving PT structures is the exposure of steel tendons to aggressive environmental conditions, particularly chloride-induced corrosion, which threatens their long-term

* Corresponding author: ahabib@sharjah.ac.ae

http://dx.doi.org/10.28991/CEJ-2025-011-06-014

performance [4]. In some cases, protective grouting materials intended to safeguard tendons contribute to corrosion issues due to variations in quality and composition. Chloride-induced corrosion is a significant concern, as it severely compromises the durability of PT concrete structures, which are integral to modern infrastructure. Exposure to chloride-rich environments accelerates deterioration, leading to premature failures that raise safety concerns and impose substantial economic burdens due to increased maintenance and repair costs [5-7]. The interaction between concrete and steel further complicates this problem, as well as the influence of environmental conditions and the effectiveness of protective measures [8]. Previous research has extensively analyzed the impact of chloride-induced corrosion on PT structures. Studies by Blomfors et al. [9] and Vereecken et al. [10] have examined the reduction in load-bearing capacity due to chloride exposure, reinforcing the urgency of developing effective corrosion management strategies. Meanwhile, research by Hu et al. [11] has focused on corrosion monitoring techniques for steel-reinforced structures, contributing to early detection and prevention efforts.

PT structures in the United Arab Emirates (UAE) face severe challenges due to harsh environmental conditions, including acid rain and elevated chloride levels [12]. High temperatures, humidity, and chloride exposure accelerate deterioration, facilitating carbonation and corrosion of steel tendons [13]. Studies on corrosion mechanisms in PT structures indicate that degradation results from multiple factors, including moisture, oxygen levels, and exposure to corrosive agents [14]. Among various corrosion types, pitting corrosion is especially concerning due to its localized and highly damaging nature, posing a serious risk of sudden tendon failures [15].

The quality of grouting materials in PT structures directly influences their susceptibility to corrosion, with variations in material composition significantly affecting the rate and severity of deterioration. The complexity of corrosion-related degradation has led to extensive academic investigation [16, 17]. This process arises from environmental and material factors contributing to steel tendon corrosion. The initiation and progression of corrosion are primarily driven by moisture, oxygen, and chloride ions, which are prevalent in coastal areas and locations where deicing salts are frequently applied [18].

Mechanical stresses inherent in prestressed structures further exacerbate corrosion. High stress levels in steel tendons accelerate corrosion processes at the anode when electrochemical conditions at the cathode facilitate reactions, leading to accelerated deterioration and structural weakening [19]. Additional environmental factors, such as temperature fluctuations and humidity variations, influence corrosion rates [20]. High temperatures accelerate chemical reactions, while elevated humidity levels provide the moisture necessary for corrosion progression [21]. The deterioration of concrete structures due to corrosion follows distinct stages, beginning with an initiation phase, during which electrolytes such as chloride-contaminated water compromise the passive protective layer of steel tendons, PT ducts, and strands [22].

The propagation phase follows, characterized by concrete cracking due to the expansion of rust layers, which reduces the effective cross-section of steel tendons and significantly weakens structural durability [23]. Factors such as concrete cover depth, steel reinforcement diameter, temperature, moisture levels, and oxygen availability directly influence the rate of corrosion [24]. Chloride ions from groundwater, seawater, precipitation, or construction materials containing chlorides can further degrade the steel's passive layer, accelerating corrosion [25].

Given the increasing prevalence of PT structures in the UAE, repair strategies must be tailored to the region's environmental conditions, exceptionally high chloride exposure, and the effects of acid rain, both accelerating structural degradation. A successful repair methodology must address immediate structural deficiencies and ensure long-term resilience against ongoing environmental challenges. Effective preservation of PT structures requires integrating environmental, material, and design considerations, particularly in extreme climates such as the UAE. Various testing methodologies assess the condition of PT elements and inform repair strategies. Nondestructive testing (NDT) techniques, including visual inspections, acoustic emission analysis, and half-cell potential measurements, provide critical data on structural integrity without causing damage [26]. Semi-destructive techniques, such as core sampling and chloride content analysis, complement these methods by offering detailed assessments of material properties and contamination levels.

Selecting repair strategies is essential for ensuring the long-term performance of rehabilitated PT structures. Standard techniques include patch repairs, electrochemical chloride extraction, and cathodic protection systems, though their effectiveness varies depending on environmental factors and the severity of deterioration [27]. Developing a durable repair framework requires a thorough understanding of local environmental conditions and the structural health of PT elements [28].

Despite extensive research on corrosion in PT structures, significant knowledge gaps remain in rehabilitating and repairing partially damaged PT structures in extreme environments [12, 29]. The combination of high temperatures, humidity, and chloride exposure in the UAE presents challenges that are not fully addressed in the existing literature.

Additionally, interactions between modern grouting materials and environmental conditions require further investigation. This study seeks to address these gaps by analyzing cases of PT structural failures caused by corrosion, identifying key deterioration mechanisms, and proposing a comprehensive repair framework. Using a case study of a corrosion-damaged PT building, this research evaluates the combined impact of environmental and material factors on PT system degradation. Through nondestructive and semi-destructive assessments, corrosion damage is quantified, and rehabilitation strategies are compared to determine an effective and sustainable repair approach. The research methodology is illustrated in Figure 1.

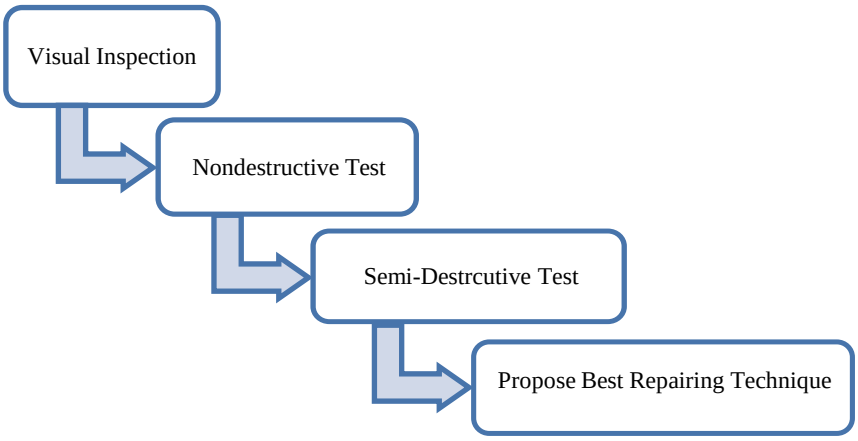

Figure 1. Flowchart showing the adopted research methodology in this study

Although previous studies have addressed the use of CFRP in rehabilitating deteriorated RC members, limited data exists on its effectiveness when integrated with epoxy crack injection, micro-concrete enlargement, and waterproofing for partially corroded PT systems. Moreover, the long-term viability of such interventions in aggressive environments is not fully established. This study addresses this gap through a real case in the UAE, where a corroded PT slab system was rehabilitated using a multi-pronged methodology. The novelty of this research lies in its integrated approach, evaluating corrosion mechanisms, identifying internal tendon degradation, and applying CFRP strengthening in combination with structural repair techniques. The effectiveness of the intervention is assessed through mechanical testing and compared with baseline values. This work contributes new insights into the practical and technical outcomes of composite rehabilitation in PT systems and provides a validated framework for durability-oriented structural recovery.

2. Case Study

This study examines a three-story (G+2) building that has exhibited significant structural deterioration after 26 years of service. The structure includes halls and office spaces on all floors, and recent inspections have revealed severe deterioration, particularly in the soffits of the roof slab. Notable signs of damage include delamination, spalling, and visible exposure of PT tendons, along with corrosion and cracking. These observations indicate reinforcement corrosion as a primary cause of structural degradation.

This case highlights the challenges associated with aging structures in corrosive environments. The findings underscore the necessity of proactive maintenance and effective repair strategies to ensure safety and functionality. A combination of nondestructive and semi-destructive testing techniques was applied to evaluate the structural condition. These methods have been widely recognized for their reliability in assessing concrete durability and deterioration over the past decades [30].

3. Assessment Methodology

A structured in-situ and laboratory testing program was implemented to assess the physical and mechanical properties of the concrete. Representative samples were collected from key structural elements for analysis and supported by NDT. The evaluation methods included core drilling for compressive strength, cover meter surveys to determine reinforcement cover, carbonation depth measurements, and corrosion assessment through half-cell potential and resistivity tests. Additionally, ultrasonic tests, chloride content analysis, and Schmidt hammer testing were conducted to assess concrete quality and the extent of deterioration. Further laboratory analysis provided insights into visual characteristics, compressive strength, density, and chloride concentration. These experimental approaches are widely adopted in civil engineering [31]. Table 1 and Figures 2 to 6 summarize the testing locations.

Table 1. Summary of testing locations

Sample ID	Location Description
1	Ground Floor Column
2	Ground Floor Column
3	First Floor Column
4	First Floor Column
5	Second Floor Column
6	Second Floor Column
7	Second Floor Column
8	Second Floor Column
9	Roof Slab - Top
10	Roof Slab - Top
11	Roof Slab - Top
12	Roof Slab - Top
13	Roof Slab - Top
C1	Roof Slab Soffit
C2	Roof Slab Soffit
C3	Roof Slab Soffit
C4*	Roof Slab Soffit
C5*	Roof Slab Soffit
C6*	Roof Slab Soffit
G1	Roof Slab PT Tendon - Soffit
G2*	Roof Slab PT Tendon - Soffit
G3*	Roof Slab PT Tendon - Soffit
G4	Roof Slab PT Tendon - Top

* Represent the visually defective locations

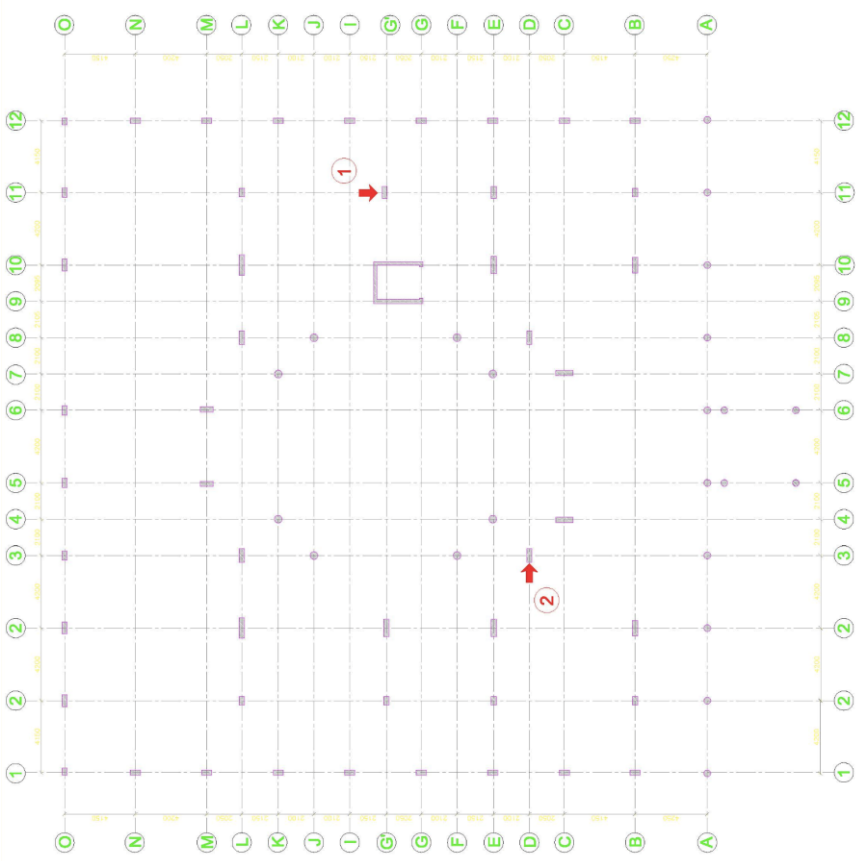

Figure 2. Ground floor test locations

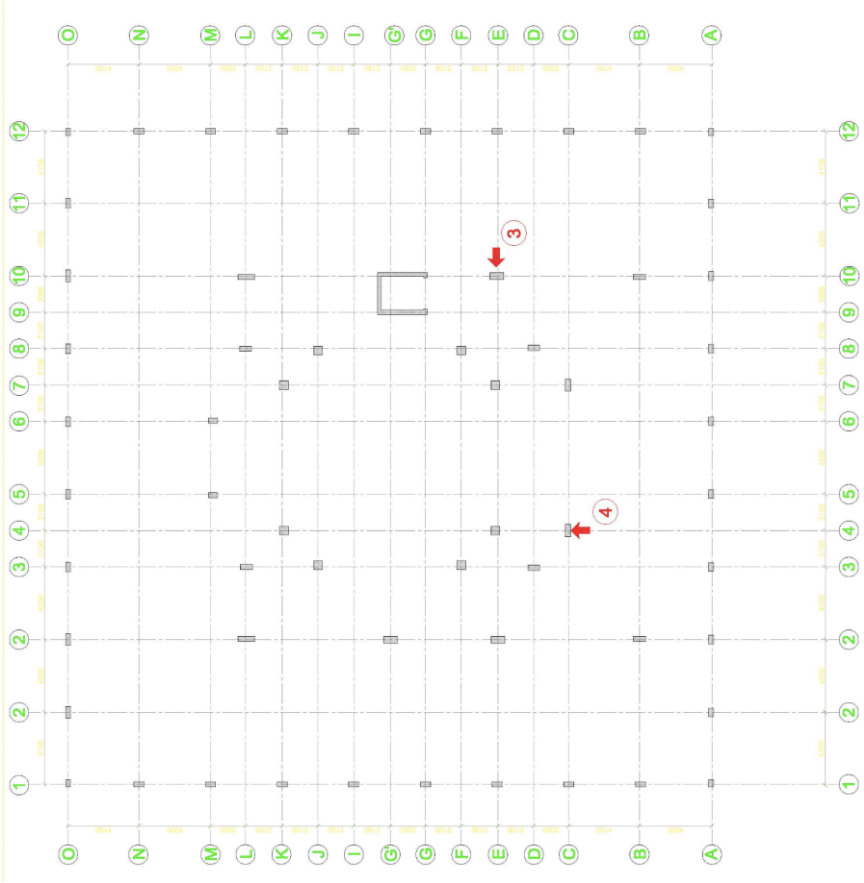

Figure 3. First-floor test locations

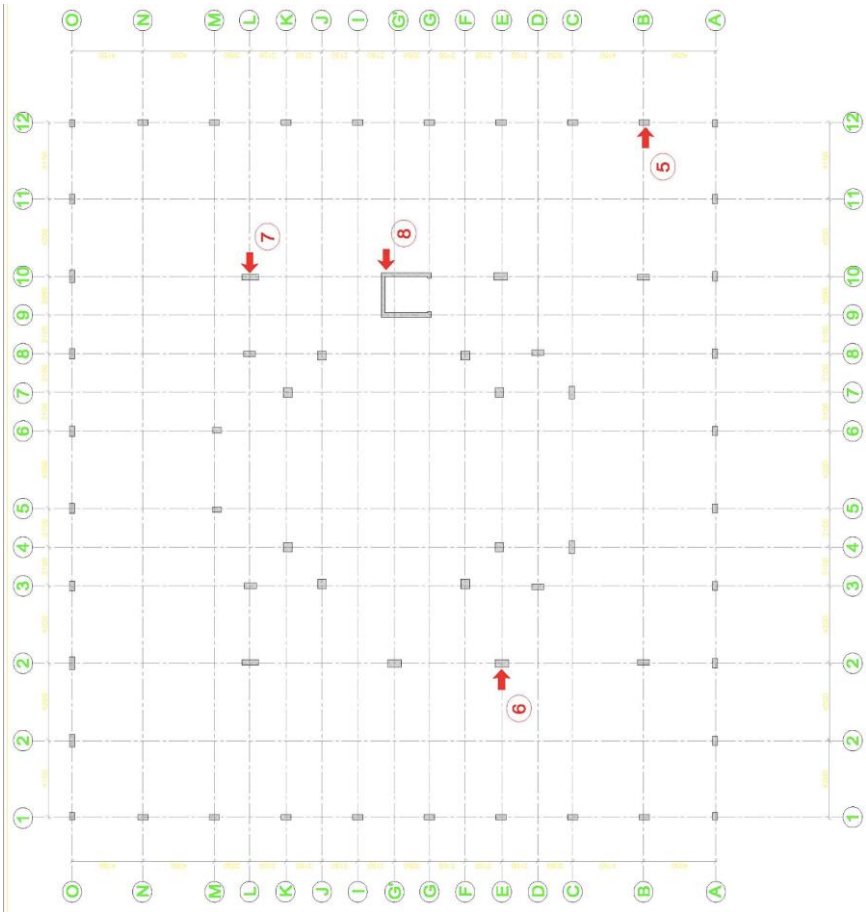

Figure 4. Second-floor test locations

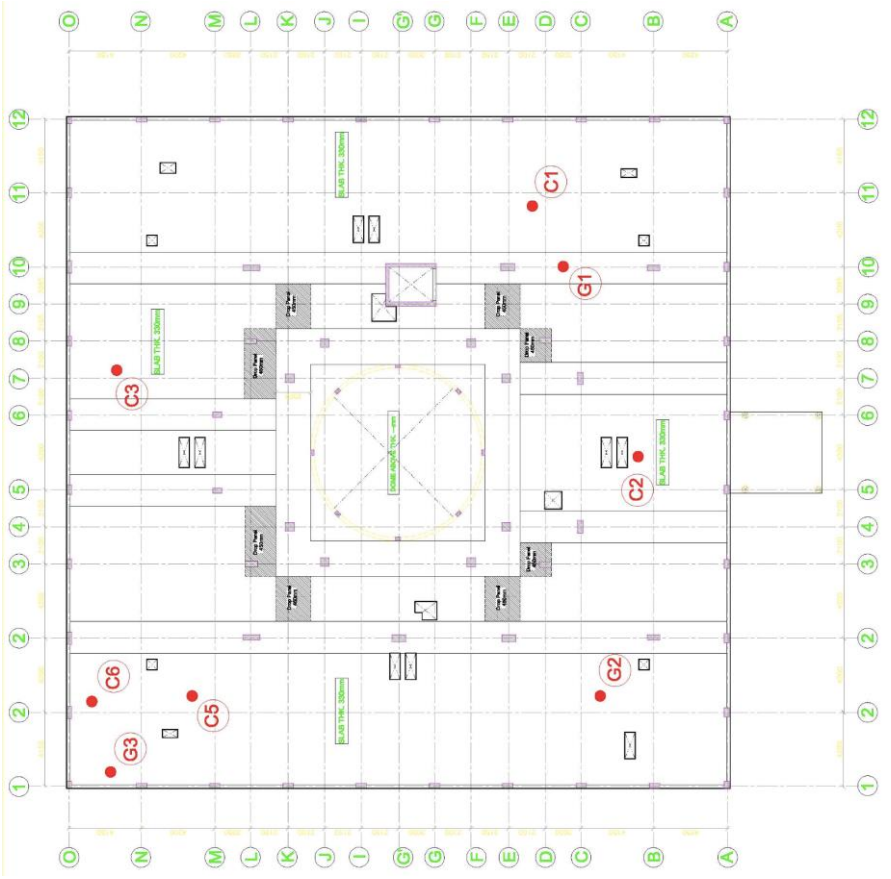

Figure 5. Roof slab soffit test locations

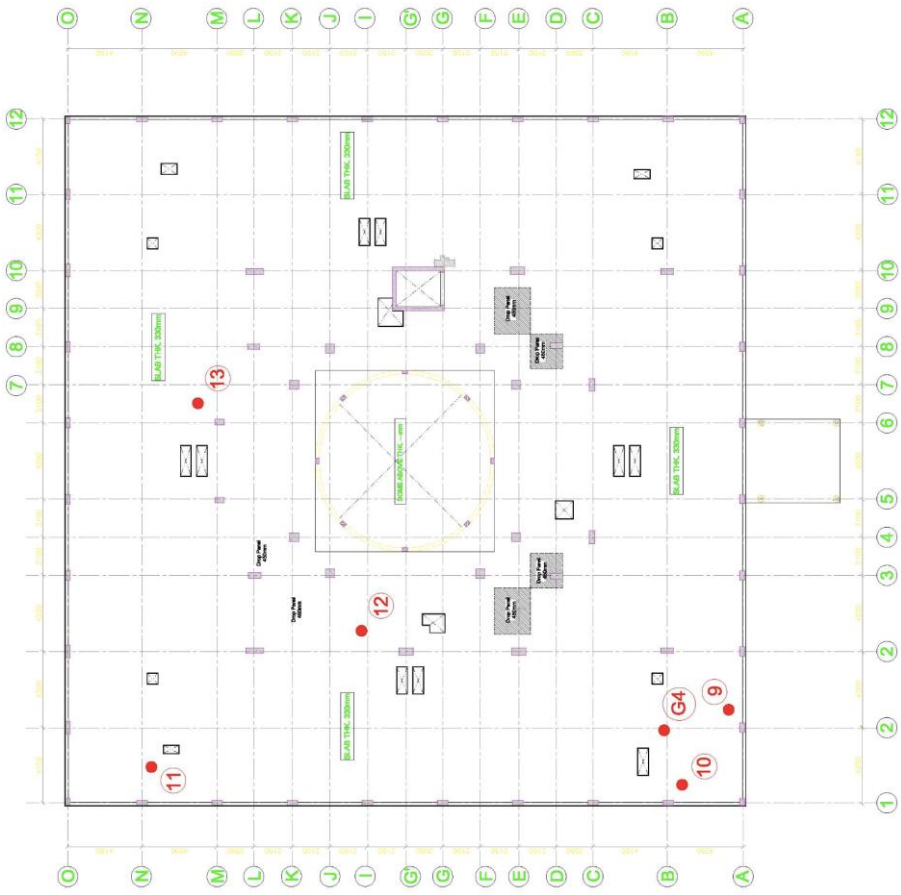

Figure 6. Roof slab test locations

4. Site Inspection Results

4.1. Visual Inspection

A detailed visual inspection and acoustic-sounding assessment were conducted across all accessible floors to evaluate the structure's condition. Each structural element was systematically examined, and observed defects were recorded. Hammer-sounding was performed by tapping concrete surfaces to detect hollow-sounding areas indicative of delamination. Figure 7 provides a typical defect markup drawing illustrating areas of deterioration.

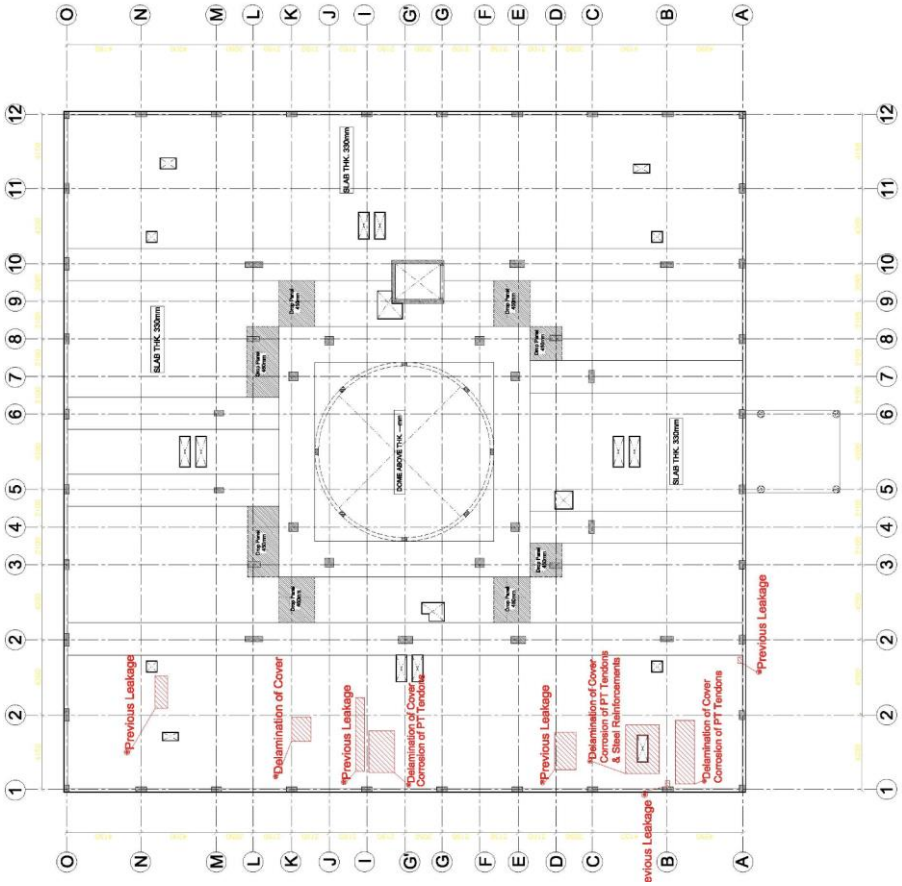

Figure 7. Condition survey of roof slab soffit (red areas show the affected slab areas)

The visual inspection identified spalling and delamination of the roof slab soffit, exposed and corroded PT ducts, and broken PT strands (Figures 8 and 9). Additionally, multiple locations showed signs of past roof leakage, parapet openings, and damaged expansion joints (Figures 10 to 12). In contrast, the first-floor slab was found to be in good condition. The findings from the visual assessment guided the selection of locations for testing.

Figure 8. Exposed and corroded PT strands at roof slab soffit

Figure 9. Delamination and spalling of exposed corroded rebar in the roof beam

Figure 10. Leakage in the roof slab

Figure 11. Delamination/spalling of the concrete in the parapet

Figure 12. Damaged expansion joint

4.2. Concrete Cover Measurement

Reinforcement covers requirements that vary across different codes of practice, which have evolved. Therefore, historical standards were considered relevant to the building's construction period and current guidelines. Although low concrete cover alone does not necessarily lead to corrosion, its role must be evaluated with carbonation and chloride test results.

A concrete cover survey was conducted on selected structural elements to determine reinforcement depth. Measurements were taken using an electromagnetic cover meter; the results are summarized in Table 2. The recorded cover values ranged from a minimum of 89 mm to a maximum of 122 mm, with an average of 102 mm at the tested locations. In all cases, the measured concrete cover exceeded the carbonation depth, which is further analyzed in this study.

Table 2. Concrete cover meter survey values

Structural element	Location No.	Cover meter survey		
		Reading (mm)		Average Reading (mm)
		Minimum	Maximum	
Roof Slab	9	98	102	100
Roof Slab	10	89	91	90
Roof Slab	11	119	122	120
Roof Slab	12	97	103	100
Roof Slab	13	99	101	100

4.3. Carbonation Depth

Codes of practice prescribe minimum reinforcement cover to prevent carbonation from reaching the reinforcement within the design life of a structural element. The extent and progression of corrosion can be evaluated by comparing the measured carbonation depths with the age of the concrete.

Carbonation depth was determined by testing freshly exposed concrete surfaces obtained through chipping a drilled hole originally used for dust sampling. A chemical indicator test was applied to assess carbonation based on the difference in alkalinity between carbonated and uncarbonated concrete. A 1% phenolphthalein solution in diluted ethyl alcohol was used as the indicator. When applied, the solution remains colorless in carbonated concrete, while uncarbonated areas turn purple-pink when the pH exceeds 10, indicating unaltered concrete. This test was performed following BS EN 14630 [32] and RILEM CPC-18 [33].

The outer carbonated layer retained its natural color upon testing, while the uncarbonated portion appeared pink. Since atmospheric carbon dioxide reacts with exposed surfaces immediately, tests were conducted on freshly exposed concrete. To maintain accuracy, care was taken to prevent contamination by dust from uncarbonated concrete. Figure 13 illustrates the carbonation depth testing process, while Table 3 presents the measured depths at the tested locations. The results indicate that the maximum carbonation depth remains below the concrete cover, suggesting minimal risk of corrosion due to carbonation.

Figure 13. Carbonation test process

Table 3. Carbonation results

Structural Element	Location No.	Carbonation (mm)	Average Cover (mm)	Protected?
Roof Slab Top	9	10	100	No
Roof Slab Top	10	10	90	Yes
Roof Slab Top	11	10	120	Yes
Roof Slab Top	12	8	100	Yes
Roof Slab Top	13	8	100	Yes

4.4. Half-Cell Potential Measurements

Corrosion in reinforced concrete is an electrochemical process that can be evaluated using electro-potential mapping, even when no visible signs of deterioration are present. The condition of embedded reinforcement is assessed by measuring electrical potentials through standard half-cell testing, provided the reinforcement maintains electrical continuity.

In this method, one terminal of a high-impedance millivoltmeter is connected to the reinforcement, while the other is linked to a half-cell electrode, such as copper/copper sulfate or silver/silver chloride, which is placed in direct contact with the concrete surface. The half-cell typically consists of a copper electrode immersed in a copper sulfate electrolyte solution, as Figures 14 and 15 illustrate. The ASTM C876 [34] standard provides guidelines for interpreting corrosion probability based on potential values. Table 4 summarizes the corrosion probability associated with these measurements.

Figure 14. Canin system for measuring potential

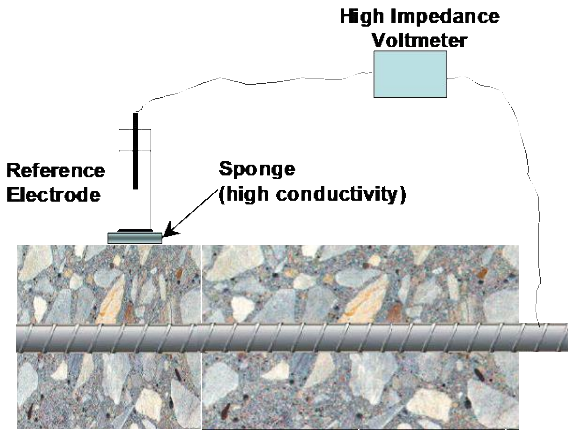

Figure 15. Schematic diagram for half-cell potential measurement

Table 4. Half-cell test results

Test No.	Minimum Reading (mV)	Maximum Reading (mV)	% Measurements < -200mV	% Measurements (-200mV to -350mV)	% Measurements > -350mV	No. of Readings
1	-371	-418	0	0	100	9
2	-271	-320	0	100	0	9
3	-338	-346	0	100	0	9
4	-346	-367	0	10	90	9
5	-229	-296	0	100	0	9
	Significance (ASTM C876-91)		**> 90% Probability of No Corrosion**	Corrosion Uncertain	> 90% Probability of Corrosion	-

A half-cell potential survey was conducted at five concrete surface locations to assess the likelihood of reinforcement corrosion. Measurements were taken using a grid-based approach, with readings recorded at 100 mm intervals. Table 4 summarizes the findings, detailing the number of readings, value ranges, and percentage distributions for each surveyed element. Since the measurements followed a uniform square grid with a predefined interval, the percentage distribution also identifies areas with more than 90% probability of no corrosion and regions where corrosion potential remains uncertain. The results indicated an uncertain probability of corrosion at most tested locations, whereas locations 1 and 4 exhibited a high probability of corrosion at the time of testing.

4.5. Electrical Resistivity Measurement of Concrete Surface

Corrosion of steel in concrete generates an electrochemical reaction, producing a current flow that leads to metal dissolution. This process allows the probability of reinforcement corrosion to be assessed by evaluating the electrical resistance of the concrete. Electrical resistivity is determined by applying current through the outer probes while measuring the potential drop between the inner probes. Resistivity values can be calculated based on current and voltage drop readings, indicating concrete quality.

Surface resistivity measurements offer significant information about the condition of concrete structures. Research has demonstrated a direct relationship between resistivity, corrosion probability, and chloride diffusion rate. Applications of this method include:

- Estimation of the corrosion rate.
- Correlation to chloride permeability.
- On-site assessment of curing efficiency.
- Determination of zonal requirements for cathodic protection systems.
- Identification of wet and dry areas in a concrete structure.
- Indication of variations in the water/cement ratios within a concrete structure.
- Identification of areas within a structure most susceptible to chloride penetration.

Correlation to water permeability of rock.

The Concrete Resistivity Meter (Figure 16) has replaced the Rapid Chloride Permeability Test and Surface Resistivity testing under ASTM C1202 [35] and AASHTO T277 standards. The Surface Resistivity test offers a quicker and more efficient method for estimating concrete permeability, serving as a viable alternative to the labor-intensive rapid chloride permeability test. The State of Louisiana has adopted this method under LATR 233.

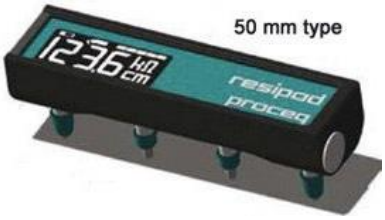

Figure 16. Concrete resistivity meter

In this procedure, an electrical current is applied through the two outer probes, while the potential difference is measured between the two inner probes. Conductivity is determined by ions present in the pore liquid, as illustrated in Figure 17. The calculated resistivity depends on probe spacing and is expressed as:

$$\rho = \frac{2\pi a V}{I} \quad (\text{k}\Omega\text{cm}) \tag{1}$$

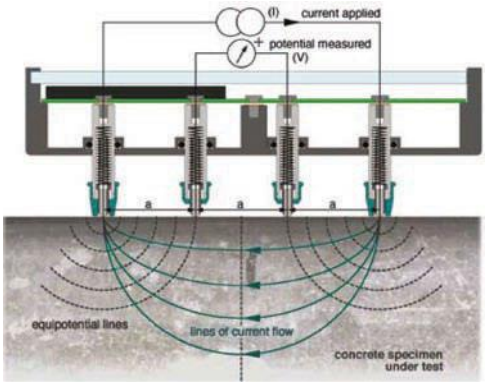

Figure 17. Concept of concrete resistivity

Table 5 provides the interpretation of resistivity measurements, which aids in assessing the likelihood of corrosion, while Table 6 presents test results from five different locations, all exhibiting high to very high corrosion rates.

Table 5. Likelihood of corrosion as a function of concrete resistivity

No.	Concrete Resistivity (ρ)	Interpretation on Corrosion
1	ρ ≥ 100 kΩcm	Corrosion is unlikely - Low corrosion rate
2	ρ = 50 to 100 kΩcm	Risk of corrosion is low - Low to moderate corrosion rate
3	ρ = 10 to 50 kΩcm	Risk of corrosion is moderate - High corrosion rate
4	ρ ≤ 10 kΩcm	Risk of corrosion is high - Very high corrosion rate

Table 6. Resistivity result

Structural Element	Location No.	Resistivity (kΩcm)
Roof Slab Top	9	3.8
Roof Slab Top	10	3.9
Roof Slab Top	11	13.8
Roof Slab Top	12	38.7
Roof Slab Top	13	24.8

4.6. Concrete Core Sampling

A total of 13 concrete cores were extracted from different locations in the building, designated as GFC1, GFC2, FFC1, FFC2, SFC1, SFC2, SFC3, SFC4, RFS1, RFS2, RFS3, RFS4, and RFS5. The coring process employed a rotary core cutting machine with hollow diamond bits cooled by fresh water. Before drilling, an electromagnetic cover meter (Ground Penetrating Radar) was used to avoid cutting through steel reinforcement. During the procedure, efforts were made to minimize damage to both the structural elements and the extracted cores.

4.7. Roof Protection System

The roof slab is protected by multiple layers, including tiles, sand filling, waterproofing, and screed, which obstruct direct visual inspection or acoustic assessment. A section was removed at a selected location to evaluate the condition of the waterproofing system and underlying concrete. The uppermost layer consists of tiles and a 50 mm sand filling. Beneath this, a 4 mm waterproofing sheet was removed to expose the concrete slab, which is coated with two screed layers of 40 mm and 50 mm thickness, respectively. Figure 18 illustrates these layers within the waterproofing system.

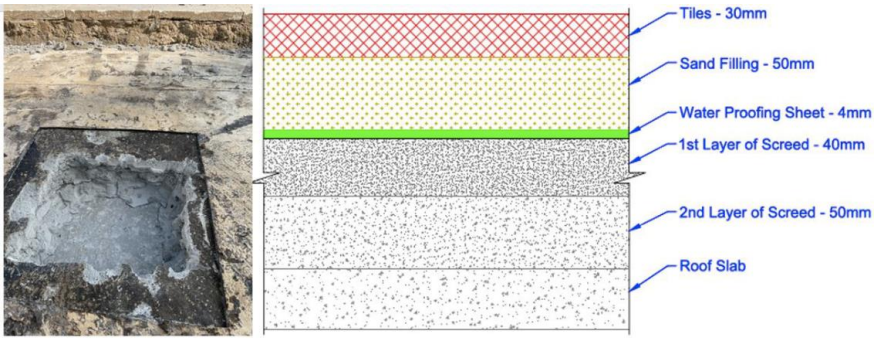

Figure 18. Roof protection system as found at the location with a section showing different layers of protection

5. Laboratory Testing Results

5.1. Compressive Strength

Thirteen concrete core samples were extracted from different locations within the building and subjected to compressive strength testing following the guidelines of BS EN 12504:1 2009 [36]. These cores, with an approximate diameter of 70 mm, were obtained using a rotary core cutting machine equipped with hollow diamond bits and cooled with fresh water. Before coring, an electromagnetic cover meter (Ground Penetrating Radar - GPR) was employed to avoid damaging reinforcement bars. Special precautions were taken to minimize potential harm to the structural elements and extracted cores.

All retrieved samples were systematically labeled, securely stored in protective containers, and transported to the laboratory for further examination. The cores underwent a series of assessments in the laboratory, including visual inspection, photographic documentation, cutting, trimming, density measurement, and compressive strength testing. These analyses provided critical data regarding the physical and mechanical properties of the concrete.

The majority of the cores exhibited medium grading with well-distributed aggregate composition. Test results, illustrated in Figure 19, show that the bulk density of the concrete cores before testing ranged from 2110 to 2230 kg/m³, with an average of 2163 kg/m³. The estimated in-situ cube strength varied between 14.1 and 28.7 N/mm², with an average strength of 20 N/mm²

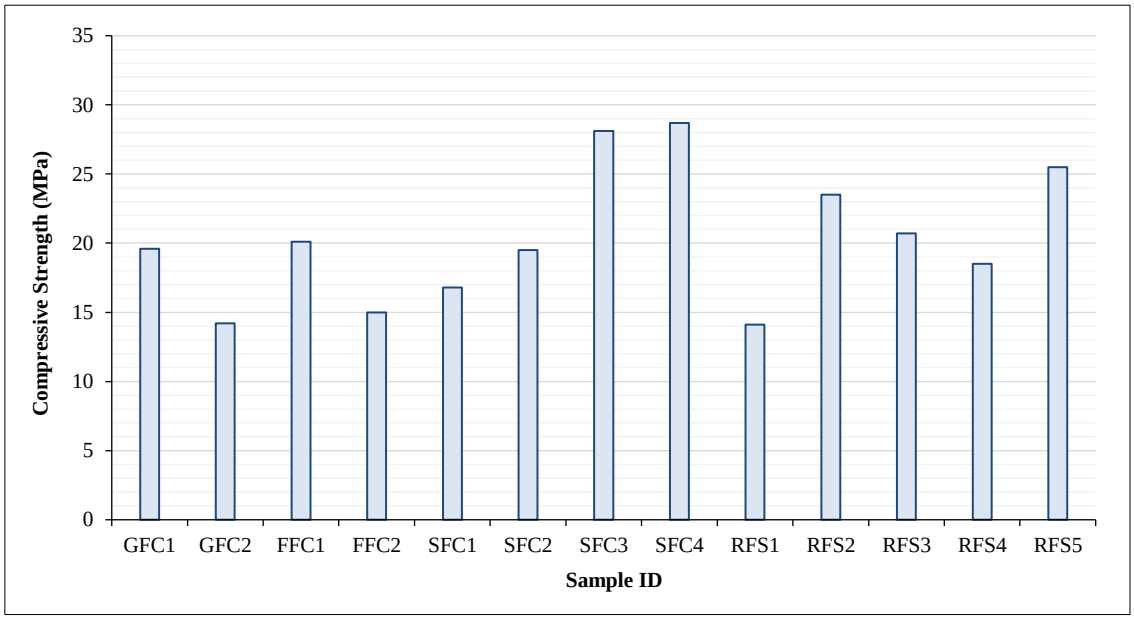

Figure 19. Summary of cube compressive strength of all elements

5.2. Chloride Ion Contamination Profiles

Dust samples were collected from 15 locations to determine the chloride content in the concrete. The chloride ion content (Cl^-) was expressed as a percentage of the total weight of the concrete samples, including aggregate. Once the cement content was established, these values were converted to chloride ion content by the weight of the cement, enabling comparisons with recommended limits outlined in practice codes. Chloride presence in concrete plays a significant role in reinforcement durability, as steel corrosion risk due to chloride contamination depends on several factors, including:

- Chloride concentration in the concrete.
- Concrete alkalinity.
- Type of cement used.
- Presence of chloride during the mixing process.
- Chloride penetration through the hardened concrete surface due to an aggressive environment.

Modern concrete specifications, such as the CIRIA Guide to the Construction of Reinforced Concrete in the Arabian Peninsula (2002), establish a maximum allowable chloride content of 0.3% for reinforced concrete made with Portland types of cement containing 4% or more C3A. OPC and ASTM Types I and II generally exceed this threshold.

The chloride content in the dust samples was determined according to BS 1881-124:2015+A1:2021 [37], with values ranging between 0.01% and 0.3% by total concrete weight. The corresponding chloride ion content by weight of cement varied between 0.06% and 0.18%, as shown in Table 7. The chloride concentration in the tested reinforced concrete elements remained within permissible limits, indicating a low risk of chloride-induced corrosion across all tested locations. Additionally, chloride content in the grout of PT tendons was measured at 0.02% and 0.03%, well below the allowable limit of 0.08% by weight of cementitious material, as specified in the AASHTO LRFD Bridge Construction Specifications (3rd edition).

Table 7. Chloride content results

Location No.	Test Location	Depth (mm)	Chloride Content (% by Wt. of Concrete)	Chloride Content (% by Wt. of Cement)
***** *The chloride contents by weight of cement were calculated using the average cement content and the received concrete density of the core specimens obtained from each location.*				
9	Roof Slab - Top	25	0.01	0.06
		50	0.01	0.06
		75	0.01	0.06
10	Roof Slab - Top	25	0.03	0.18
		50	0.02	0.12
		75	0.01	0.06
11	Roof Slab - Top	25	0.02	0.12
		50	0.01	0.06
		75	0.01	0.06
12	Roof Slab - Top	25	0.01	0.06
		50	0.01	0.06
		75	0.01	0.06
13	Roof Slab - Top	25	0.02	0.12
		50	0.01	0.06
		75	0.01	0.06
C1	Roof Slab - Soffit	25	0.02	0.12
		50	0.01	0.06
		75	0.01	0.06
C2	Roof Slab - Soffit	25	0.03	0.18
		50	0.02	0.12
		75	0.01	0.06
C3	Roof Slab - Soffit	25	0.03	0.18
		50	0.01	0.06
		75	0.01	0.06
C4*	Roof Slab - Soffit	25	0.02	0.12
		50	0.01	0.06
		75	0.01	0.06
C5*	Roof Slab - Soffit	25	0.02	0.12
		50	0.01	0.06
		75	0.01	0.06
C6*	Roof Slab - Soffit	25	0.03	0.18
		50	0.02	0.12
		75	0.01	0.06
G1	Roof Slab PT Tendon - Soffit	-	0.02	-
G2*	Roof Slab PT Tendon - Soffit	-	0.03	-
G3*	Roof Slab PT Tendon - Soffit	-	0.02	-
G4	Roof Slab PT Tendon - Top	-	0.02	-

Site inspections and laboratory test results confirm that corrosion occurs in areas identified with delamination and seemingly intact concrete surfaces. The primary contributing factors to this deterioration are loss of alkalinity and prolonged exposure to moisture. If alkalinity depletion or moisture infiltration persists, further corrosion risk exists in structurally sound areas. Repairing the waterproofing system is essential to protect the concrete surface and prevent further water ingress.

The roof slab is deemed structurally unsafe due to severe corrosion in the PT tendons and steel reinforcements, increasing the likelihood of sudden concrete cover delamination and posing a public safety hazard. Structural strengthening of the roof slab is necessary; however, reinforcing it would introduce additional loads on the roof beams, compromising their integrity. Therefore, both the roof slab and supporting beams must be strengthened to ensure overall structural safety. Given the inadequate compressive strength of the vertical elements, a comprehensive structural assessment of the building columns is required to determine their sufficiency. These findings underscore the urgent need for remedial measures to maintain structural stability and ensure the building's long-term durability.

5.3. Summary of the Laboratory Testing Results

The following are the main findings from the laboratory tests:

- Visual inspection identified spalling, concrete delamination, corroded PT ducts, and broken PT strands on the soffit of the roof slab.
- Evidence of multiple prior leaks, parapet openings, and damaged expansion joints was observed while the first-floor slab remained in good condition.
- Significant moisture penetration and water staining were detected across multiple sections of the roof soffit slab.
- Concrete delamination and cracking were noted in ground floor columns at gridline A/2, attributed to rebar corrosion.
- Compressive strength testing indicated values ranging from 14.1 to 28.7 N/mm², with an average of 20 N/mm², falling below the expected design strength and revealing structural inadequacies.
- Chloride concentration in reinforced concrete elements remained within permissible limits, indicating a low risk of chloride-induced corrosion.
- Carbonation depth measurements confirmed no risk of carbonation-induced corrosion.
- Half-cell potential assessments indicated a high probability (above 90%) of no active corrosion, though certain areas presented uncertain corrosion potential.
- Electrical resistivity tests revealed high to very high corrosion rates across all tested locations.

6. Repair and Rehabilitation Strategy

The case study presented in this paper highlights significant durability challenges in PT concrete structures, with water ingress identified as the primary factor contributing to deterioration. This issue, particularly affecting steel strands, is a major concern in structural engineering and concrete technology. A detailed investigation and analysis reveal the complexity of concrete degradation in PT systems, emphasizing the interaction between environmental factors, material properties, and facility management practices that contribute to structural deterioration. The findings confirm that corrosion of embedded steel within PT ducts and reinforcement is the primary cause of degradation, aligning with prior research that attributes steel corrosion in concrete to water infiltration, which initiates the corrosion process [38]. However, this study presents a more complex deterioration scenario. Laboratory tests, including half-cell potential measurements, carbonation depth analysis, and chloride contamination assessments, indicated relatively low risk, yet localized PT slab deterioration was still observed. Affected areas exhibited significant water penetration from shafts and openings, with no corrective measures. Additionally, severe water leakage from the HVAC system was detected in the same deteriorated roof sections. These findings suggest that moisture exposure and oxygen availability are critical in initiating and accelerating corrosion beyond the slab deterioration [39].

The structural damage was widespread, with the roof slab soffit experiencing the most severe deterioration. Observations showed that 25% of the inspected roof slab soffit areas exhibited delamination or spalling, as illustrated in Figure 7. Additionally, all PT ducts and strands in this region displayed visible signs of corrosion. In contrast, the ground, first, and second-floor slabs remained relatively good. Several factors contributed to this pattern of damage. The roof slab, more exposed to environmental conditions, suffered more significant deterioration than interior structural elements. Failures in the waterproofing system facilitated water infiltration, accelerating slab degradation. Concrete quality also played an important role, as compressive strength tests indicated that none of the samples met the design strength of 30 MPa.

The measured values ranged between 14.1 and 28.7 N/mm², with an average of 20 N/mm². This lower compressive strength likely increased permeability and reduced protection against corrosion. These findings highlight the necessity of repair strategies that address visible structural damage and restore concrete's structural capacity and protective properties to prevent further deterioration.

Environmental conditions were found to significantly influence the corrosion process, particularly the effects of condensation and water leakage from air conditioning units in accelerating structural deterioration. These findings align with previous studies [38, 40], which established that fluctuating wet and dry conditions can substantially increase the corrosion rate in reinforced concrete. This study extends that understanding by examining PT structures and demonstrating how environmental exposure, combined with high chloride levels in the grouting material, creates an environment highly conducive to PT strand corrosion.

The visual survey and test data confirm that corrosion extends beyond surface-level concerns to deeper structural integrity issues. The severe corrosion observed in PT ducts and strands, leading to delamination and spalling, is a well-documented indicator of advanced deterioration. Addressing the root causes of corrosion and restoring structural capacity is critical, rather than merely treating visible damage. This approach aligns with modern repair methodologies emphasizing a comprehensive understanding of deterioration mechanisms to develop effective repair and mitigation strategies [41].

The study also examines the fundamental components of corrosion in reinforced concrete, steel, water, and oxygen, as widely documented in existing literature [42]. However, this case study offers a focused assessment of how these factors interact specifically within PT structures exposed to severe environmental conditions, contributing to a broader understanding of concrete durability. Given the variation in environmental exposures, the observed corrosion rates underscore the necessity of context-specific assessments when evaluating corrosion risks in PT structures.

A thorough evaluation of restoration strategies was conducted, considering the advantages and limitations of each approach. Patch repairs, while cost-effective and relatively simple to implement, provide limited durability and often require frequent replacement. Additionally, they do not address the issue of inadequate structural capacity, leaving the underlying problem unresolved. In contrast, complete reconstruction of deteriorated sections, combined with protective coatings, provides a more robust long-term solution by resolving immediate structural deficiencies and improving corrosion resistance. Optimal performance and durability require selecting the most suitable repair approach based on a detailed structural assessment.

For rehabilitating PT concrete structures, an integrated strategy is necessary to effectively address visible and latent deterioration. This process begins with validating as-built drawings using advanced nondestructive techniques such as ground penetrating radar (GPR), which ensures accurate structural integrity assessments and informs necessary repairs [43]. Additionally, modeling the structure using its existing compressive strength data is essential for evaluating safety and continued usability for occupants.

The structural analysis results indicate that the roof slab is unsafe due to extensive PT tendons and corrosion caused by steel reinforcement. This deterioration presents a significant risk, as it may lead to the sudden delamination of the concrete cover, posing a safety hazard. The required strengthening of the roof slab would increase the load on the roof beams, potentially affecting their stability. Therefore, reinforcing the roof slab and beams is necessary to ensure overall structural integrity. Given the low compressive strength of the vertical elements, the building's columns should also be strengthened.

Several strengthening strategies were evaluated, and a targeted approach was implemented to restore the building while maintaining its structural integrity. A combination of techniques was employed to achieve this objective. The beams were enlarged from the top and strengthened with CFRP at the bottom to preserve the building’s aesthetics. The slab, having a thickness less than that of the beams, was enlarged from the bottom by adding a reinforcement layer. Additionally, columns with low compressive strength were enlarged to enhance their load-bearing capacity.

Figure 20 illustrates the strengthening strategies in an elevation section, while Figures 21 to 24 present the detailed strengthening design of the roof slab in plan views. The primary criterion for selecting this approach was ensuring long-term durability. CFRP was chosen due to its well-documented effectiveness in enhancing the load-bearing capacity of PT concrete elements.

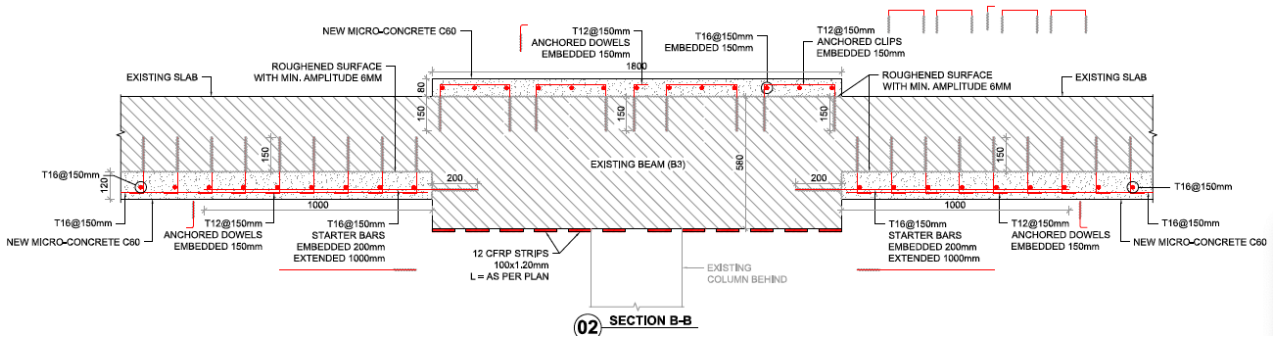

Figure 20. Elevation for beam top/bottom strengthening

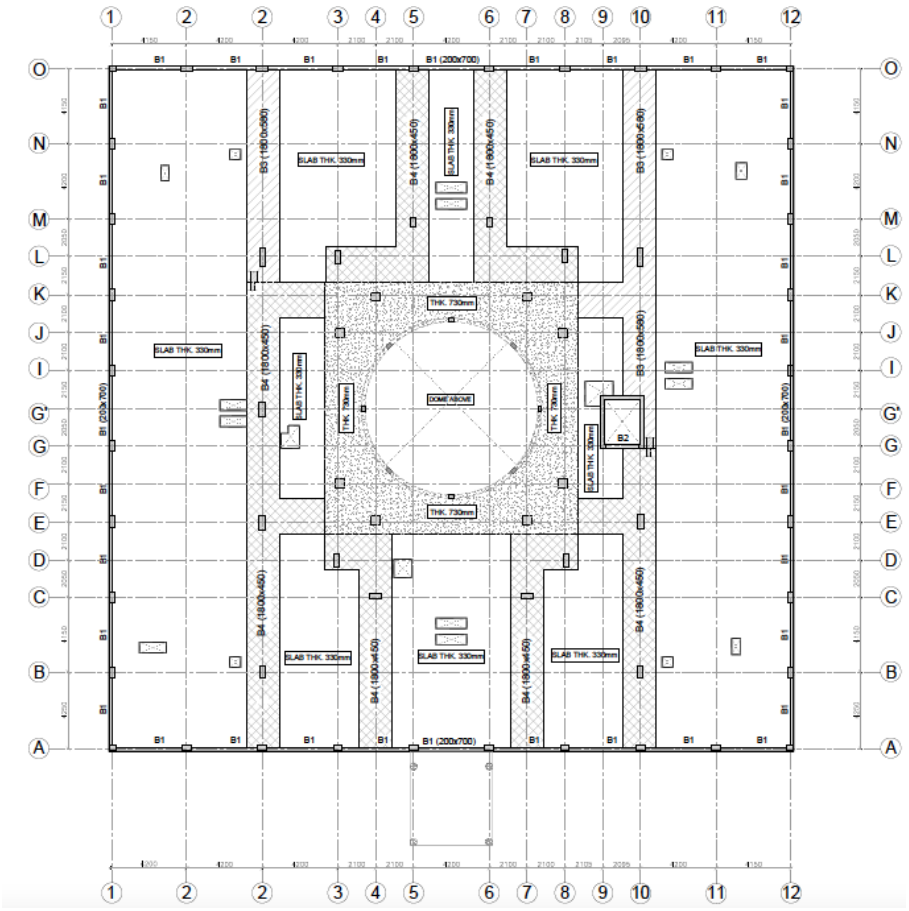

Figure 21. As-built roof slab layout

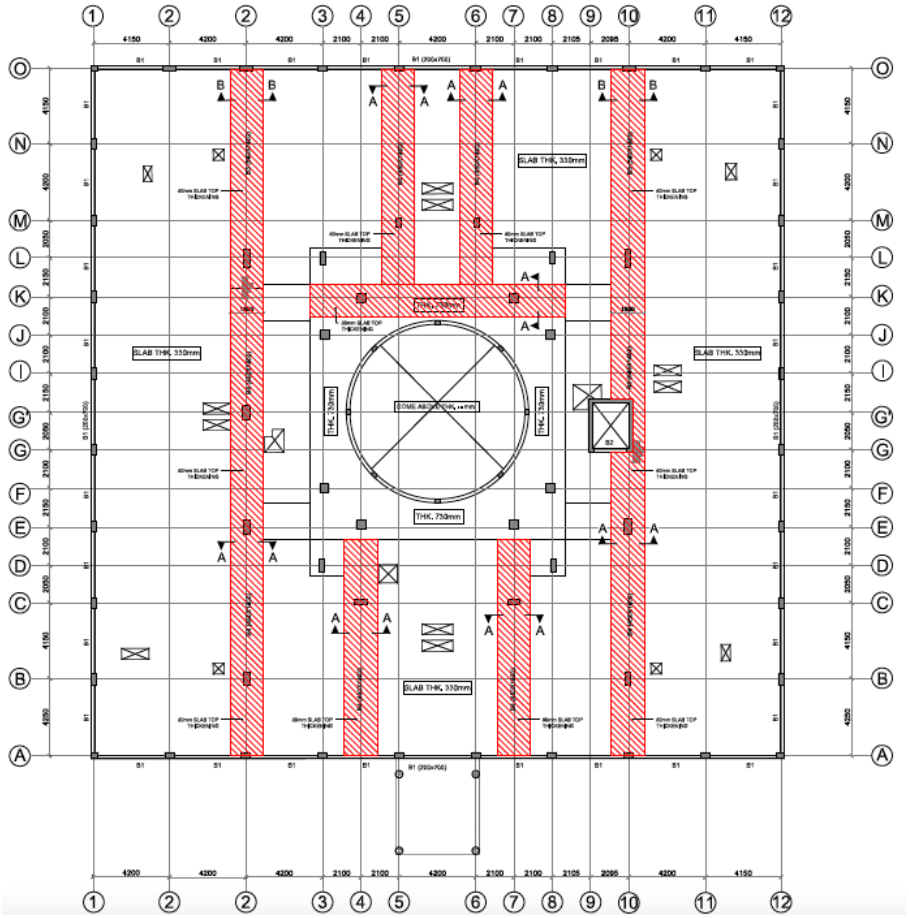

Figure 22. Roof slab top strengthen layout

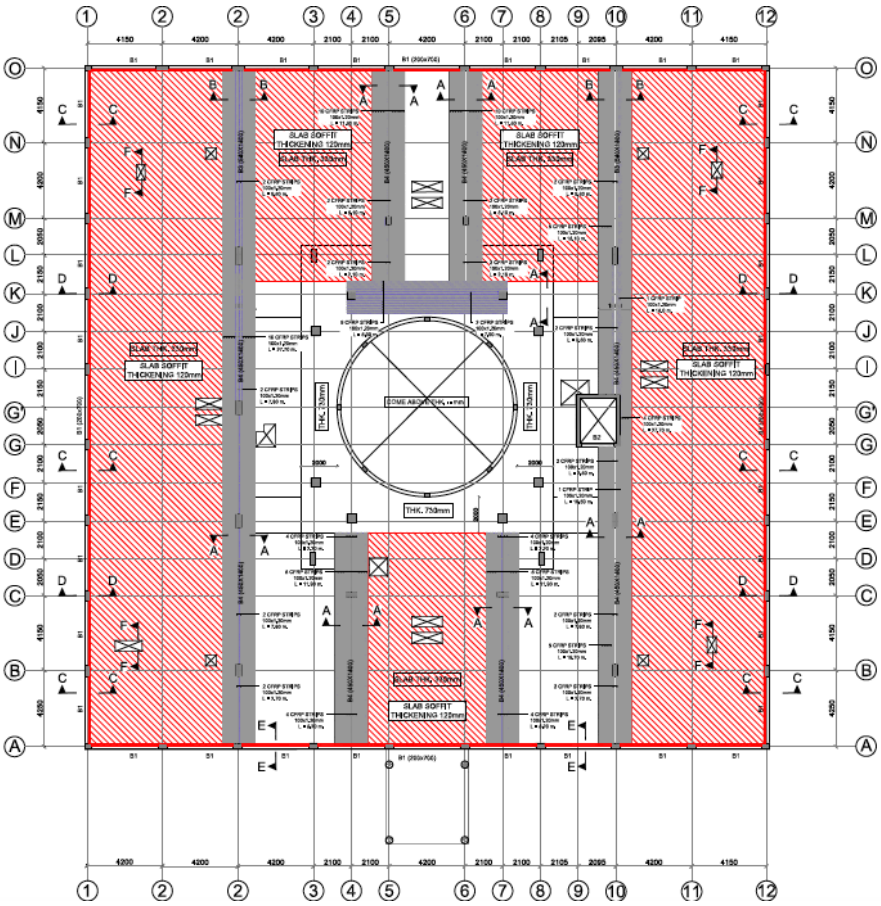

Figure 23. Roof slab bottom strengthen layout

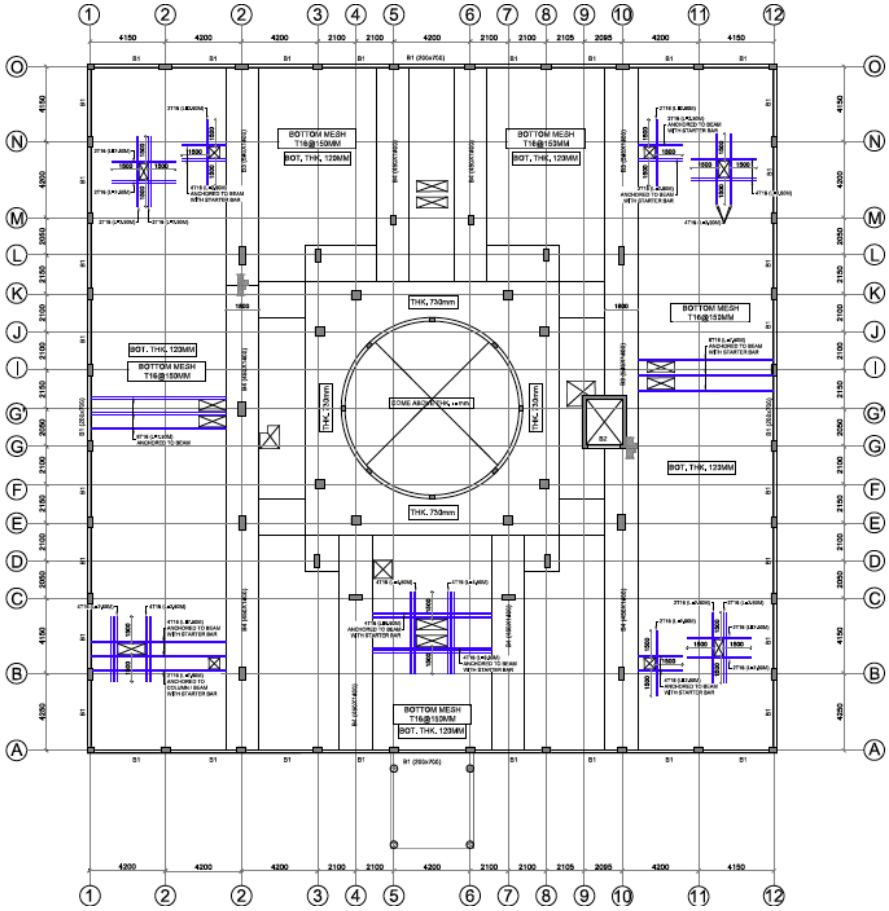

Figure 24. Roof slab bottom reinforcement detail

The slab was strengthened by enlarging it from the bottom with a 120 mm thick layer of micro-concrete having a compressive strength of 60 MPa. Prior to casting, the existing concrete surface was roughened to a depth of 6 mm to enhance the bond between the old and new concrete. The added layer was reinforced with 16 mm diameter bars placed at 150 mm spacing in both directions. Anchorage bars were embedded into the existing slab at a depth of 150 mm from the top surface and 200 mm from the slab edge to ensure proper load transfer.

Similarly, the beam was enlarged by adding an 800 mm thick layer of 60 MPa micro-concrete, reinforced with 16 mm bars spaced at 150 mm intervals. The reinforcement was secured using 12 mm diameter dowels placed at 150 mm spacing, anchored 150 mm from the bottom and 200 mm from the beam side. Additionally, the beam was externally strengthened with 12 CFRP strips, each measuring 100 mm in width and 1.2 mm in thickness, to enhance its flexural capacity.

The findings indicate that strengthening the slab section with a single CFRP layer resulted in a 30% increase in flexural strength and a 23% reduction in crack width compared to the control specimen. In accordance with ACI standards, micro-concrete was used in all enlargement locations to ensure long-term durability [44].

Additionally, crack repair in concrete and block walls was done using epoxy injections and 'V' groove techniques. These methods extend beyond simple surface filling, as they restore the material's impermeability to moisture, a critical factor in preventing further deterioration. A waterproofing process was also undertaken, involving removing previous failed systems and the application of advanced waterproofing technologies. Combined with proper maintenance of roof drainage systems, this approach not only repaired existing damage but also protected the structure from future water-related deterioration. Beyond immediate repairs, long-term corrosion protection remains essential. Protective coatings were applied to limit oxygen penetration at the steel rebar interface, significantly reducing corrosion and preventing further water infiltration.

In addition to the experimental findings, several practical and economic considerations were observed during the rehabilitation process. Although the current study primarily focuses on the short-term evaluation of the rehabilitation strategy, provisions for long-term durability monitoring have been incorporated into the post-rehabilitation maintenance plan. These include periodic resistivity assessments, corrosion potential mapping, and scheduled visual inspections. The effectiveness of the waterproofing system was verified following the intervention using waterproofing test and handheld moisture meters at representative locations, with no evidence of residual moisture detected. The selection of CFRP application zones was informed by a detailed condition assessment, including corrosion profiling and structural inspections, and was limited to areas exhibiting critical deterioration. Surface preparation procedures involved mechanical abrasion and the application of epoxy bonding agents to ensure adequate adhesion between CFRP and the concrete substrate; subsequent visual evaluations confirmed a uniform bond with no signs of debonding or surface failure. Furthermore, a brief cost comparison has been included to contextualize the adopted CFRP rehabilitation approach relative to alternative methods, such as steel plate bonding and sectional replacement. Challenges encountered during on-site installation, particularly in zones with restricted access, were mitigated by segmenting the CFRP into smaller components and employing adaptable application techniques, ensuring precise and effective implementation.

7. Conclusions

This study provides a comprehensive assessment of the deterioration and rehabilitation of partially corroded post-tensioned (PT) concrete structures, focusing on a real-world case study in the United Arab Emirates. Through a rigorous evaluation involving nondestructive and semi-destructive testing, the research identifies chloride-induced corrosion as the primary cause of structural degradation, exacerbated by environmental exposure and inadequate waterproofing measures. The findings emphasize the necessity of implementing advanced rehabilitation techniques to restore the structural integrity of PT systems and prolong their service life. Key conclusions drawn from this study include:

- The investigation confirms that the deterioration of the PT structure resulted primarily from moisture ingress, chloride contamination, and carbonation-induced steel corrosion. The highest levels of degradation were observed in PT ducts and strands, particularly in areas where waterproofing had failed. Laboratory and field assessments indicate that corrosion progression significantly reduces the structural capacity of affected elements, necessitating targeted repair and strengthening interventions.
- The application of carbon fiber-reinforced polymer (CFRP) proved to be a viable solution for strengthening corroded PT structures. Experimental findings demonstrate that CFRP reinforcement enhanced the flexural strength of the slab by 30% and reduced crack width by 23%, thereby improving both mechanical performance and long-term durability. This outcome aligns with existing research supporting CFRP’s effectiveness in mitigating corrosion-related deterioration in PT elements.
- A systematic approach integrating structural repairs, CFRP strengthening, and advanced waterproofing techniques was adopted to ensure long-term structural resilience. The rehabilitation plan included removing corroded material, enlarging critical load-bearing components, and applying protective coatings. Additionally, micro-concrete was used in all enlargement locations to enhance durability in compliance with ACI standards.

- The proposed rehabilitation framework offers a sustainable solution for extending the service life of PT concrete structures exposed to aggressive environments. By addressing both immediate damage and underlying deterioration mechanisms, the strategy minimizes future maintenance requirements and enhances the building's resilience against environmental stressors. The integration of CFRP reinforcement, epoxy crack injection, and improved waterproofing measures ensures effective corrosion mitigation and structural longevity.
- While the adopted methodology demonstrated significant improvements in structural performance, further research is needed to refine rehabilitation techniques for PT structures under varying environmental conditions. Future investigations should focus on optimizing CFRP application techniques, evaluating the long-term behavior of rehabilitated structures under sustained loads, and exploring alternative strengthening materials to enhance cost-effectiveness and performance.

8. Declarations

8.1. Author Contributions

Conceptualization, H.A., A.H., Z.A., M.M., S.A., S.B., and M.J.; methodology, H.A., A.H., Z.A., M.M., S.A., S.B., and M.J.; validation, H.A., A.H., Z.A., M.M., S.A., S.B., and M.J.; formal analysis, H.A., A.H., Z.A., M.M., S.A., S.B., and M.J.; investigation, H.A., A.H., Z.A., M.M., S.A., S.B., and M.J.; resources, S.A., M.M., and Z.A.; data curation, H.A. and A.H.; writing—original draft preparation, H.A., A.H., and A.M.; writing—review and editing, H.A., Z.A., A.H., and A.M.; visualization, H.A. and A.H.; supervision, M.M., S.A., and Z.A.; project administration, M.A., S.A., Z.A., and S.B.; funding acquisition, M.A., S.A., and Z.A. All authors have read and agreed to the published version of the manuscript.

8.2. Data Availability Statement

The data presented in this study are available on request from the corresponding author.

8.3. Funding

The authors received no financial support for the research, authorship, and/or publication of this article.

8.4. Conflicts of Interest

The authors declare no conflict of interest.

9. References

[1] Ahmad, O. (2022). Financial comparative study between post-tensioned and reinforced concrete flat slab. International Journal of Advanced Engineering, Sciences and Applications, 3(1), 1–6. doi:10.47346/ijaesa.v3i1.67.

[2] Yousif, S., & Saka, M. P. (2021). Optimum design of post-tensioned flat slabs with its columns to ACI 318-11 using population-based beetle antenna search algorithm. Computers and Structures, 256, 106520. doi:10.1016/j.compstruc.2021.106520.

[3] Mohan, M. K., Pillai, R. G., Santhanam, M., & Gettu, R. (2021). High-performance cementitious grout with fly ash for corrosion protection of post-tensioned concrete structures. Construction and Building Materials, 281, 122612. doi:10.1016/j.conbuildmat.2021.122612.

[4] Lu, Z. H., Wu, S. Y., Tang, Z., Zhao, Y. G., & Li, W. (2021). Effect of chloride-induced corrosion on the bond behaviors between steel strands and concrete. Materials and Structures/Materiaux et Constructions, 54(3), 1–16. doi:10.1617/s11527-021-01724-8.

[5] Yang, Z. N., Lu, Z. H., Li, C. Q., Liu, X., & Song, X. (2024). Effect of grouting quality on flexural behavior of corroded post-tensioned concrete T-beams. Case Studies in Construction Materials, 21. doi:10.1016/j.cscm.2024.e03766.

[6] Nürnberger, U. (2002). Corrosion induced failure mechanisms of prestressing steel. Materials and Corrosion, 53(8), 591-601. doi:10.1002/1521-4176(200208)53:8<591::AID-MACO591>3.0.CO;2-X.

[7] Menga, A., Kanstad, T., Cantero, D., Bathen, L., Hornbostel, K., & Klausen, A. (2023). Corrosion-induced damages and failures of posttensioned bridges: A literature review. Structural Concrete, 24(1), 84–99. doi:10.1002/suco.202200297.

[8] Kioumarsi, M., Benenato, A., Ferracuti, B., & Imperatore, S. (2021). Residual flexural capacity of corroded prestressed reinforced concrete beams. Metals, 11(3), 442. doi:10.3390/met11030442.

[9] Blomfors, M., Lundgren, K., & Zandi, K. (2021). Incorporation of pre-existing longitudinal cracks in finite element analyses of corroded reinforced concrete beams failing in anchorage. Structure and Infrastructure Engineering, 17(7), 960-976. doi:10.1080/15732479.2020.1782444.

[10] Vereecken, E., Botte, W., Lombaert, G., & Caspeele, R. (2021). Assessment of corroded prestressed and posttensioned concrete structures: A review. Structural Concrete, 22(5), 2556–2580. doi:10.1002/suco.202100050.

[11] Hu, J. Y., Zhang, S. S., Chen, E., & Li, W. G. (2022). A review on corrosion detection and protection of existing reinforced concrete (RC) structures. Construction and Building Materials, 325, 126718. doi:10.1016/j.conbuildmat.2022.126718.

[12] Lau, K., Permeh, S., & Lasa, I. (2023). Corrosion of prestress and posttension reinforced concrete bridges. Corrosion of Steel in Concrete Structures, Woodhead Publishing, Sawston, United Kingdom. doi:10.1016/B978-0-12-821840-2.00013-4.

[13] Ding, Z., & Cao, Q. (2024). A state-of-the-art review of flexural behaviors of PC beams with corroded prestressing tendons. Structures, 63, 106430. doi:10.1016/j.istruc.2024.106430.

[14] Campione, G., & Zizzo, M. (2022). Influence of strands corrosion on the flexural behavior of prestressed concrete beams. Structures, 45, 1366–1375. doi:10.1016/j.istruc.2022.09.073.

[15] Vecchi, F., Franceschini, L., Tondolo, F., Belletti, B., Sánchez Montero, J., & Minetola, P. (2021). Corrosion morphology of prestressing steel strands in naturally corroded PC beams. Construction and Building Materials, 296, 123720. doi:10.1016/j.conbuildmat.2021.123720.

[16] Asp, O., Tulonen, J., Kuusisto, L., & Laaksonen, A. (2021). Bond and re-anchoring tests of post-tensioned steel tendon in case of strand failure inside cement grouting with voids. Structural Concrete, 22(4), 2373–2390. doi:10.1002/suco.202000351.

[17] Huang, D., Chen, P., Peng, H., Yang, Y., Yuan, Q., & Su, M. (2021). A review and comparison study on drying shrinkage prediction between alkali-activated fly ash/slag and ordinary Portland cement. Construction and Building Materials, 305, 124760. doi:10.1016/j.conbuildmat.2021.124760.

[18] Kim, J., & Song, J. (2021). Time-Dependent Reliability Assessment and Updating of Post-tensioned Concrete Box Girder Bridges Considering Traffic Environment and Corrosion. ASCE-ASME Journal of Risk and Uncertainty in Engineering Systems, Part A: Civil Engineering, 7(4), 4021062. doi:10.1061/ajrua6.0001188.

[19] Peng, J., Xiao, J., Yang, Y., Dong, Y., & Zhang, J. (2024). Long-term experimental study and prediction of the mechanical performance on corroded prestressing steel strands subjected to marine salt spray environment. Construction and Building Materials, 425, 136069. doi:10.1016/j.conbuildmat.2024.136069.

[20] Cai, Z. K., Yuan, W., Li, S., Pan, X., & Zheng, Z. (2025). Seismic fragility analysis of coastal bridges considering different corrosion damage modes among multiple RC bridge columns. Case Studies in Construction Materials, 22, 4099. doi:10.1016/j.cscm.2024.e04099.

[21] Yang, J., Yuan, Z., Liu, J., & Yu, S. (2023). Study on Lifetime Performance Evaluation of a Precast Prestressed Concrete Frame in Chloride Environments. Materials, 16(20), 6666. doi:10.3390/ma16206666.

[22] Googan, C. (2022). Marine Corrosion and Cathodic Protection. In Marine Corrosion and Cathodic Protection. CRC Press. doi:10.1201/9781003216070.

[23] Jouni, A. (2024). A comprehensive approach about the cracks in post-tensioned bridges and case study. Ph.D. Thesis, Politecnico di Torino, Torino, Italy.

[24] Asamoto, S., Sato, J., Okazaki, S., Chun, P. J., Sahamitmongkol, R., & Nguyen, G. H. (2021). The cover depth effect on corrosion- induced deterioration of reinforced concrete focusing on water penetration: Field survey and laboratory study. Materials, 14(13), 3478. doi:10.3390/ma14133478.

[25] Asmara, Y. P. (2024). Concrete Reinforcement Degradation and Rehabilitation: Damages, Corrosion and Prevention. Springer Nature, Singapore. doi:10.1007/978-981-99-5933-4.

[26] Hassani, S., & Dackermann, U. (2023). A Systematic Review of Advanced Sensor Technologies for Non-Destructive Testing and Structural Health Monitoring. Sensors, 23(4), 2204. doi:10.3390/s23042204.

[27] Rincon, L. F., Moscoso, Y. M., Hamami, A. E. A., Matos, J. C., & Bastidas-Arteaga, E. (2024). Degradation Models and Maintenance Strategies for Reinforced Concrete Structures in Coastal Environments under Climate Change: A Review. Buildings, 14(3), 562. doi:10.3390/buildings14030562.

[28] Hao, H., Bi, K., Chen, W., Pham, T. M., & Li, J. (2023). Towards next generation design of sustainable, durable, multi-hazard resistant, resilient, and smart civil engineering structures. Engineering Structures, 277, 115477. doi:10.1016/j.engstruct.2022.115477.

[29] Li, F., Luo, X., & Liu, Z. (2017). Corrosion of anchorage head system of post- tensioned prestressed concrete structures under chloride environment. Structural Concrete, 18(6), 902-913. doi:10.1002/suco.201600140.

[30] Tešić, K., Baričević, A., & Serdar, M. (2021). Non-destructive corrosion inspection of reinforced concrete using ground-penetrating radar: A review. Materials, 14(4), 1–20. doi:10.3390/ma14040975.

[31] Al Houri, A., Habib, A., Elzokra, A., & Habib, M. (2020). Tensile testing of soils: History, equipment and methodologies. Civil Engineering Journal, 6(3), 591–601. doi:10.28991/cej-2020-03091494.

[32] BS EN 14630:2006. (2006). Products and systems for the protection and repair of concrete structures. Test methods. Determination of carbonation depth in hardened concrete by the phenolphthalein method. British Standards Institution (BSI), London, United Kingdom.

[33] RILEM CPC-18. (1988). Measurement of Hardened Concrete Carbonation Depth. Materials and Structures 21, 453–455. doi:10.1007/BF02472327.

[34] ASTM C876. (2015). Standard test method for corrosion potentials of uncoated reinforcing steel in concrete. ASTM International, Pennsylvania, United States.

[35] ASTM C1202. (2012). Standard Test Method for Electrical Indication of Concrete's Ability to Resist Chloride Ion Penetration. ASTM International, Pennsylvania, United States.

[36] BS EN 12504-1:2009. (2000). Testing concrete in structures - Cored specimens. Taking, examining and testing in compression. British Standards Institution (BSI), London, United Kingdom.

[37] BS 1881-124:2015+A1:2021. (2021). Testing Concrete - Methods for analysis of hardened concrete. British Standards Institution (BSI), London, United Kingdom.

[38] Funahashi, M., & Young, W. T. (1996). Cathodic protection of prestressed bridge members—Full-scale testing. Transportation research record, 1561(1), 13-25. doi:10.1177/0361198196156100103.

[39] Hansson, C. M. (1984). Comments on electrochemical measurements of the rate of corrosion of steel in concrete. Cement and Concrete Research, 14(4), 574–584. doi:10.1016/0008-8846(84)90135-2.

[40] Permeh, S., & Lau, K. (2022). Review of Electrochemical Testing to Assess Corrosion of Post-Tensioned Tendons with Segregated Grout. Construction Materials, 2(2), 70–84. doi:10.3390/constrmater2020006.

[41] Hauashdh, A., Nagapan, S., Jailani, J., & Gamil, Y. (2024). An integrated framework for sustainable and efficient building maintenance operations aligning with climate change, SDGs, and emerging technology. Results in Engineering, 21, 101822. doi:10.1016/j.rineng.2024.101822.

[42] Poursaee, A., & Hansson, C. M. (2009). Potential pitfalls in assessing chloride-induced corrosion of steel in concrete. Cement and Concrete Research, 39(5), 391–400. doi:10.1016/j.cemconres.2009.01.015.

[43] ACI 228.1R-19. (2019). Report on Methods for Estimating In-Place Concrete Strength. American Concrete Institute (ACI), Farmington Hills, United States.

[44] ACI. (2003). RAP-5: Surface Repair Using Form-and-Pump Techniques. American Concrete Institute (ACI), Farmington Hills, United States.